buildings

MDPI

Article

Exploring the Dual Nature of Olive Husk: Fiber/Aggregate in Lightweight Bio-Concrete for Enhanced Hygrothermal, Mechanical, and Microstructural Properties

Halima Belhadad [1,2,*], Nadir Bellel [1] and Ana Bras [2,*]

[1] Energy Physics Laboratory (EPL), Faculty of Exact Sciences, University Constantine 1, Route Ain El Bey, Constantine 25000, Algeria; bellelnadir@umc.edu.dz
[2] Built Environment and Sustainable Technologies (BEST) Research Institute, School of Civil Engineering and Built Environment, Liverpool John Moores University, Liverpool L3 3AF, UK
* Correspondence: belhadadhalima@outlook.fr (H.B.); a.m.armadabras@ljmu.ac.uk (A.B.)

Abstract: This study investigates the potential of thermally treated olive husk (OH)—a heterogeneous agro-industrial by-product comprising olive stones, pulp, and fibrous residues—as a multifunctional component in lightweight bio-concrete. Uniquely, this work harnesses the intrinsic dual nature of OH as both a fibrous reinforcement and a porous aggregate, without further fractionation, to evaluate its influence on the hygrothermal and mechanical behavior of cementitious composites. While prior studies have often focused selectively on thermal conductivity, this work provides a comprehensive assessment of all major thermal parameters; including diffusivity, effusivity, and specific heat capacity; offering deeper insights into the full thermal behavior of bio-based concretes. OH was incorporated at 0%, 10%, and 20% by weight, and the resulting concretes were subjected to a comprehensive characterization of their thermal, hygric, mechanical, and microstructural properties. Thermal performance metrics included conductivity, specific heat capacity, diffusivity, effusivity, time lag, and predicted energy savings. Hygric behavior was assessed through the moisture buffering value (MBV), while density, porosity, and mechanical strengths were also evaluated. At 20% OH content, thermal conductivity decreased to 0.405 W/m·K (a 72% reduction), thermal diffusivity dropped by 87%, and thermal effusivity reached 554 $W \cdot s^{0.5}/m^2 \cdot K$, collectively enhancing thermal inertia and increasing the time lag by 77% (to 2.32 h). MBVs improved to 2.18 $g/m^2 \cdot \%RH$, rated as "Excellent" for indoor moisture regulation. Despite the higher porosity, the bio-concrete maintained adequate mechanical integrity, with compressive and flexural strengths of 11.68 MPa and 3.58 MPa, respectively, attributed to the crack-bridging action of the fibrous inclusions. Microstructural analysis (SEM/XRD) revealed improved paste continuity and denser C–S–H formation, attributed to enhanced matrix compatibility following oil removal via thermal pre-treatment. These findings demonstrate the viability of OH as a new bio-based, multifunctional additive for fabricating thermally efficient, hygroscopically active, and structurally sound concretes suitable for sustainable construction.

Keywords: olive husk; bioconcrete; valorization; hygro; thermal performance

Academic Editor: Pavel Reiterman

Received: 30 April 2025
Revised: 21 May 2025
Accepted: 29 May 2025
Published: 4 June 2025

Citation: Belhadad, H.; Bellel, N.; Bras, A. Exploring the Dual Nature of Olive Husk: Fiber/Aggregate in Lightweight Bio-Concrete for Enhanced Hygrothermal, Mechanical, and Microstructural Properties. *Buildings* **2025**, *15*, 1950. https://doi.org/10.3390/buildings15111950

1. Introduction

The environmental impact of traditional construction materials has driven a global shift toward sustainable alternatives. Among these, concrete—one of the most widely used building materials—plays a major role in carbon dioxide emissions, resource depletion,

and waste production [1]. The construction sector alone accounts for nearly 36% of global energy consumption and approximately 37% of greenhouse gas emissions [2,3], underscoring the urgent need for eco-friendly innovations in building materials. In response, lightweight concrete (LWC) has emerged as a viable alternative, offering reduced structural loads, improved energy efficiency, and lower material consumption. Notably, projects such as the Wabash River Bridge have demonstrated the potential of LWC, achieving a 17% reduction in structural density and a cost saving of 18% (approximately USD 1.7 million) [4]. Despite these benefits, conventional LWC often underperforms in hygrothermal regulation; specifically in managing moisture uptake, water retention, and thermal insulation. Most (LWC) formulations depend on synthetic or mineral-based aggregates that reduce density but fail to improve humidity buffering or thermal behavior [5]; an omission of critical importance, considering that approximately 40% of building energy consumption is associated with space heating and cooling, much of which is exacerbated by inadequate moisture and thermal regulation [6].

Bio-based lightweight concrete (bio-LWC) offers a sustainable alternative to traditional concrete by reducing structural dead loads and thereby, enabling slimmer structural elements and material savings. Beyond weight reduction, bio-LWC significantly enhances thermal insulation, a critical factor in cutting building energy demand for heating and cooling. Crucially, bio-LWC goes beyond density reduction by harnessing the hygroscopic nature of natural bio-aggregates to regulate moisture exchange and buffer indoor humidity swings. Conventional LWC relies on closed-pore mineral aggregates (e.g., expanded clay, perlite, and pumice stone [7]) that reduce density but provide minimal moisture buffering, often leading to mold growth, thermal bridging, and condensation. In contrast, bio-LWC harnesses the hygroscopic nature of plant-based aggregates to actively regulate moisture exchange and buffer indoor humidity fluctuations. A substantial body of research has explored the use of plant-based aggregates in lightweight concrete, leveraging their natural porosity and hygroscopic properties to enhance hygrothermal performance, including hemp shiv [8–10], flax [11–14], straw [15–17], date palm fibers [18–21], and rice husks [22–26] each contributing low thermal conductivity (<0.30 W/m·K) and reduced bulk density (<1200 kg/m^3) [27]. Their intrinsic capillarity and sorption isotherms enable moisture buffer values (MBVs) above 2 g/(m^2·%RH), classifying them as "very good" humidity regulators [9,28–31], By contrast, ordinary and cellular concretes record MBV values of only 0.35 and 0.96 g/(m^2·%RH), respectively, both considered negligible in moisture regulation [32]. This superior hygric performance directly correlates with energy savings; for example, hempcrete formulations have demonstrated up to a 45% reduction in heating energy use, directly attributed to moisture buffering [32].

Raw olive husk (OH), the lignocellulosic by-product of olive oil extraction, represent an abundant yet largely untapped resource for bio-lighstweight concrete. For every ton of olives processed, traditional three-phase and two-phase extraction methods generate roughly 400–800 kg of wet pomace (35–60% moisture) alongside 200 kg of oil, while up to 35 kg of dry olive oil cake and 100 L of wastewater are produced per 100 kg of olives [33]. Global olive oil output reached over 2.56 million metric tons in 2023/24, while the estimate for the 2024/25 crop year shows production reaching 3.37 t [34]; 90% of which originates from Spain, Italy, Greece, Turkey, Tunisia, Morocco, and Portugal; resulting in millions of tons of residual husks and vegetation waters each year [35,36]. When mismanaged, these by-products can harm soil microbiota, aquatic ecosystems, and air quality [37]. Therefore, valorizing OH offers both environmental and economic benefits.

Among the resulting by-products, olive stones (OSs)—also termed olive pits or bones—are the dense endocarps remaining after oil extraction and separation from the rest of the fibrous material. Olive husk (OH), in contrast, refers to the fibrous, semi-porous residue composed of crushed olive bones, pulp, and skin, while olive pomace (OP), also known as

wet pomace [38], is a heterogeneous mixture of OH and olive mill wastewater, characterized by a heterogeneous blend of olive stones, woody twigs, skin, pulp remnants, and trace oil residues. Raw OH naturally contains 40–49% [39] fibrous material and exhibits low bulk density (420–640 kg/m^3) and thermal conductivity (<0.08 W/m·K) [23,40]. Its semi-high porosity lends it lightweight aggregate properties [23], and OH presents significant potential as a lightweight aggregate that could improve both the thermal efficiency and sustainability of concrete. These features position OH as a promising candidate for dual-functionality in bio-LWC applications.

Several olive oil by-products have been investigated for their potential integration into construction materials, driven by the need for sustainable alternatives to conventional aggregates and binders. Among these, olive stones (OBs) have been most extensively studied as partial sand replacements in mortar and concrete formulations. Substituting 30% of sand with OBs, for instance, has been shown to reduce bulk density by 15%, while maintaining over 70% of compressive strength [41]. OB additions ranging from 5% to 30% have also been used in stabilized bricks, reducing thermal conductivity from 1.05 to 0.60 W/m·K and compressive strength from 14.18 MPa to 10.24 MPa [42]. Other studies have reported that 100% sand replacement with OBs can yield a thermal conductivity of 0.326 W/m·K and a compressive strength of 9.58 MPa. One investigation assessed the use of wet olive pomace (a composite of OH and mill wastewater) as an additive in fired clay bricks [43], reporting an optimum compressive strength of 40.22 MPa and a thermal conductivity of 0.72 W/m·K at 10% replacement. In parallel, olive pomace fly ash (OPFA) has been explored as a supplementary cementitious material, demonstrating acceptable pozzolanic reactivity and improved environmental profiles [44–47].

Despite these findings, the use of raw, unsegregated olive husk (OH) remains underexplored—particularly with regard to its dual composition comprising both fibrous material and granular olive stones. While olive stones are typically favored in the literature for their particle uniformity and compatibility with cementitious matrices [40,48–51], their compact structure limits their ability to enhance porosity and can result in marginal improvements to thermal or hygric performance [32,52]. In contrast, OH's fibrous morphology suggests the potential to improve hygrothermal performance through microporous structures, though this remains poorly characterized in current research. However, OH's implementation may been hindered by concerns over its residual oil content (4.5–9% [33]). At the microstructural level, residual oil interferes with the hydration of cementitious matrices by forming hydrophobic films around cement particles, which hinder water access and ion exchange, thereby retarding the nucleation and growth of calcium silicate hydrate (C-S-H) phases; a phenomenon observed in oil-contaminated aggregates [53].

The intrinsic synergy between OH's fibrous strands and its porous aggregates can yield a composite that balances mechanical resilience with hygrothermal performance. While olive stone mortars suffer compressive strength losses of ~70% at 30% substitution with CEM I 42.5/52.5 [41], the fibrous network in OH is capable of micro-crack bridging, as demonstrated in fiber-reinforced concretes [54], and thus, mitigating the brittleness and reducing strength penalties. Equally important, OHs' moisture-related behavior—vital for humidity regulation, condensation control, and indoor air quality—has never been quantified for any olive-waste derivative. By contrast, hempcrete reported an MBV of 2.2 g/(m^2·%RH) [55], yet the hygrothermal potential of OH remains unreported. To date, the literature remains narrowly focused on mechanical–thermal trade-offs [40,41,43,56] overlooking OHs' high cellulose content (25–36% [36]) and microporous architecture, both of which suggest superior moisture buffering compared with conventional mineral aggregates (e.g., expanded clay).

The present study aims to bridge the critical knowledge gaps by developing an innovative lightweight concrete incorporating thermally treated olive husk (OH), without any further fractionation, thereby preserving its intrinsic dual structure as both a fibrous reinforcement and a porous aggregate. Unlike the previous studies that have focused predominantly on either the thermal conductivity or the mechanical properties of olive waste-based composites, this research investigates how the naturally coexisting fibrous and porous features of OH influence a broader set of performance parameters, including hygric regulation and crack-bridging potential. The applied thermal treatment was specifically designed to remove residual oils while retaining the internal structure of OH, thus enhancing its chemical and mechanical compatibility with cementitious matrices. This dual-functionality has not been previously exploited to assess simultaneous improvements in thermal, hygric, and mechanical behavior.

Accordingly, this study delivers a comprehensive multi-parameter characterization of the resulting bio-based lightweight concrete (bio-LWC). In contrast to most of the existing literature that limits thermal assessment to conductivity alone, this work provides a detailed thermal profile—including thermal conductivity, specific heat capacity, thermal diffusivity, thermal effusivity, time lag, and predicted energy savings—thereby offering a more holistic understanding of the material's thermophysical performance. Hygroscopic behavior is evaluated through the moisture buffering value (MBV), while mechanical integrity is assessed via compressive and flexural strength tests. Microstructural and mineralogical insights are obtained through SEM and XRD, elucidating fiber–matrix interactions, microcrack bridging effects, and the influence of thermal treatment on cement hydration. Collectively, this multifaceted investigation introduces a novel valorization pathway for unfractionated olive husk in sustainable construction and advances the state of knowledge on the integrated hygrothermal–mechanical performance of bio-based concretes.

2. Materials and Methods

2.1. Materials

The olive husk (OH) used in this study were sourced from an olive oil processing facility, obtained through a two-phase extraction method. To enhance its compatibility with cementitious matrices while preserving its dual role as both fiber and aggregate, the OH underwent a boiling pretreatment for four hours. This process effectively removed residual oils, which can interfere with cement hydration, while maintaining the fibrous and particulate components of the material. Following this treatment, the OH was characterized in accordance with the RILEM Technical Committee 236-BBM guidelines for bio-based building materials [27]. The bulk density was determined using a standard volumetric method, while particle size distribution was assessed via dry sieving (presented in Figure 1). Thermal conductivity and water absorption W∞ were also determined under controlled conditions. The porosity of the olive husk particles was derived from the bulk and specific densities [57]. Specific density was measured using a helium gas pycnometer (ULTRAPYC 1200e V5.06, QUANTACHROME, Boynton Beach, FL, USA), Profcontrol, Schonwalde-Glien, Germany in accordance with ASTM D4892 standards [58]. Oil residue, which can significantly influence binder adhesion and thermal behavior, was also analyzed using a Soxhlet extraction method (SOXTEC FOSS 2043). The total fiber content was assessed using a FIBERTEC 1020, Gemini lab, Apeldoorn, The Netherland. The key physicochemical properties and characteristics of the OH are presented in Table 1, while Figure 1 illustrates the particle size distribution of both the olive husk and sand used in this study, and Figure 2 represent its XRD analysis.

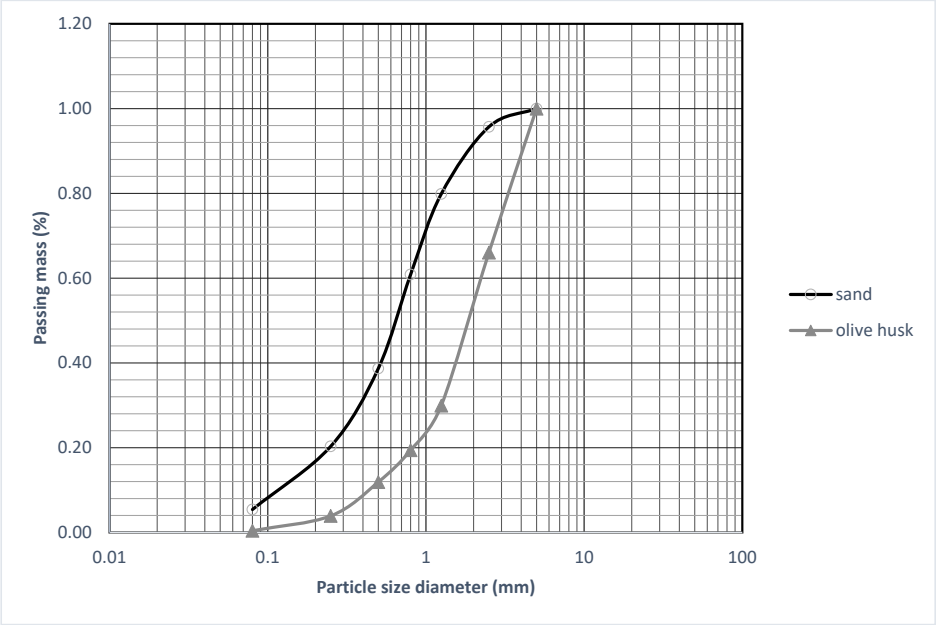

Figure 1. Particle size distribution of sand and olive husk.

Table 1. Olive husk characteristics.

Bulk Density ρ_{bulk} (kg/m^3)	598.04
True density ρ_{true}(kg/m^3)	1301.7
Total porosity (%)	54.1
Thermal conductivity λ W/(m K)	0.0812
Fiber content (%)	42.26%
Water absorption Wœ (%)	54.46
Oil residues (%)	1–1.6
Ash (%)	0.4

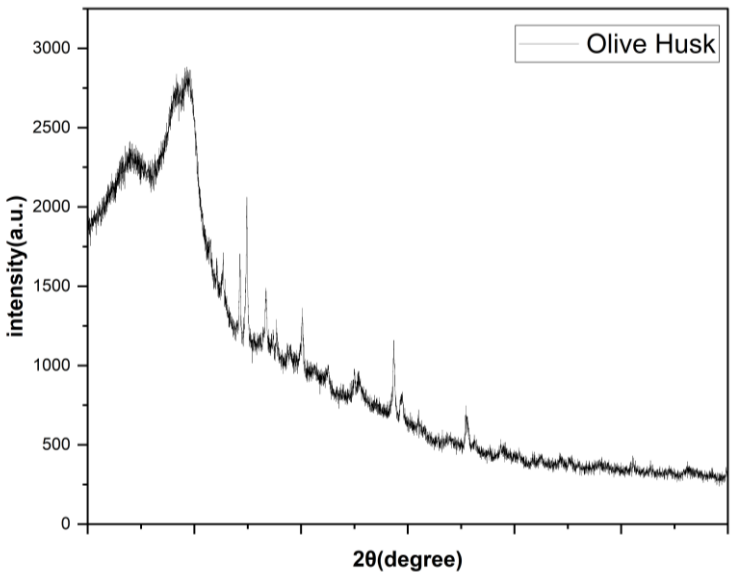

Figure 2. XRD analysis of olive husk.

The binder employed was Portland cement (CEM II/A-P 42.5 N), its chemical composition is presented in Table 2, the cement was selected for its mechanical performance and compatibility with bio-based aggregates.

Table 2. The chemical composition of Portland cement (CEM II/A-P 42.5 N).

Elements	CaO	SiO_2	Al_2O_3	Fe_2O_3	MgO	SO_3	MnO
wt. %	66.7	23.1	5.6	0.3	3.2	0.8	0.3

2.1.1. Material Selection and Composition

The bio-based lightweight concrete used in this study was developed after preliminary testing to identify an optimal 10–20% olive husk (OH) content, chosen based on favorable thermal and mechanical performance. The final formulation consists of the following:

- 62% Portland cement (CEM II/A-P 42.5 N);
- 28–18% sand;
- 10–20% olive husk (by weight).

This composition achieves a balance between mechanical strength and thermal insulation, aligning with the RILEM classification standards for lightweight concrete [55].

2.1.2. Pre-Treatment and Fabrication

The hydrophilic nature of olive husk poses a challenge for its use as a lightweighting agent in concrete. To address this, a thermal pre-treatment was applied. This process effectively removes oil residues to a minimum average of 1–1.4%, increasing surface roughness and enhancing bonding with the cement matrix which can improve mechanical performance and preventing long-term degradation in lightweight concrete. The thermal treatment was chosen for its ability to preserve the intrinsic fiber/aggregate composition of the OH. The treatment process involved the following:

- Boiling for 4 h in a 0.1 OH-to-water ratio;
- Drying in an air oven for 48 h at 60 °C; as presented in Figure 3 below.
- Pre-soaking the OH in water prior to mixing to ensure accurate cement/water proportions.

Figure 3. Treatment procedures of olive husk.

Following preparation; as presented in Table 3; the cement–sand–OH mixture was then cast into molds to produce different specimen geometries for specific tests:

- Cylindrical samples (110 × 20 mm): Used for thermal conductivity measurements following ASTM D7984. And an MBV test following the NORDEST project protocol.
- Prismatic samples (160 × 40 × 40 mm): Used for bulk and true density determination (ASTM D4892) and mechanical performance tests (compressive and flexural strength) in accordance with BS EN 196-1. As presented in Figure 4 below.

Table 3. Mix design for bio-based LWC samples (by weight).

Samples	Cement (g)	Sand (g)	Olive Husk (OH) (g)	W/B
BLC0	620	380	-	0.45
BLC10	620	280	100	0.45
BLC20	620	180	200	0.45

Figure 4. Bio-concrete specimens with 0%, 10%, and 20% olive husk content cast in different molds immediately after mixing.

Three sample types were evaluated:

- BLC0: Control sample without olive husk;
- BLC10: Bio-concrete with 10% olive husk;
- BLC20: Bio-concrete with 20% olive husk.

2.2. Methods

After casting, specimens were sealed with plastic sheets for 24 h to prevent early moisture loss, then demolded and air-cured under controlled laboratory conditions (23 ± 2 °C, 56 ± 5% RH) until testing. All tests were conducted under the same conditions to ensure consistency and reflect the standard indoor environment in which such materials typically perform.

2.2.1. Bulk, True Density and Porosity

The bulk density (ρ_{bulk}) of the samples was determined by measuring their dimensions using a precision caliper, while the true density (ρ_{true}) was measured with a ULTRAPYC 1200-e helium gas pycnometer (Quantachrome, Boynton Beach, FL, USA) in accordance with ASTM D4892 standards [58]. The total porosity (Φ) was then calculated using the following equation [57]:

$$\Phi = 1 - \frac{\rho_{bulk}}{\rho_{true}} \quad (1)$$

where Φ is the total porosity in %; ρ_{bulk} is the bulk density in kg/m^3; and ρ_{true} is the true (apparent) density in kg/m^3.

2.2.2. Thermal Properties, Thermal Time Lag, and Energy Savings Assessment

For each composition, thermal measurements were carried out on three distinct samples. On each sample, the ISOMET heat flow meter equipped with contact probe API 210412 was configured to perform three consecutive readings, and the average value was reported to enhance measurement reliability. This device enables the precise evaluation of thermal conductivity (λ), thermal diffusivity (α), and volumetric heat capacity (Cv), with a stated accuracy of ±5% in accordance with ISO 9869-1:2014 [59]. Additional thermal properties, including specific heat capacity (Cp) and thermal effusivity (E), were later

calculated. Specific heat capacity was calculated from the measured density and volumetric heat capacity using the following equation:

$$Cp = Cv/\rho \quad (2)$$

where Cp is the specific heat capacity; ρ is density; and Cv is volumetric heat capacity.

The thermal diffusivity (m^2/s), calculated as follows:

$$\alpha = \lambda/(\rho Cp) \quad (3)$$

Additionally, the thermal effusivity was calculated as follows:

$$E = \sqrt{}(\rho.Cp.\lambda) \quad (4)$$

Here, λ denotes the thermal conductivity (W/m·K); ρ is the bulk density (kg/m^3); and Cp is the specific heat capacity (J/kg·K). The volumetric heat capacity (ρ·Cp) reflects the material's ability to store thermal energy.

The thermal time lag (φ) represents the delay between peak external temperature and the corresponding peak internal temperature within a building element. This parameter is crucial for understanding the thermal inertia of construction materials, which influences indoor thermal comfort and energy efficiency. The time lag was calculated using the following equation derived from one-dimensional transient heat conduction theory:

$$\varnothing = L^2/(\pi^2\alpha) \quad (5)$$

where

Φ is the time lag (s);

L is the wall thickness (m); and

α alpha is the thermal diffusivity (m^2/s)

Here, λ denotes the thermal conductivity (W/m·K); ρ is the bulk density (kg/m^3); and Cp is the specific heat capacity (J/kg·K). The volumetric heat capacity (ρ·Cp) reflects the material's ability to store thermal energy. By substituting the calculated thermal diffusivity into the time lag equation, we determined the time lag for each specimen. The resulting time lag values were converted from seconds to hours for practical interpretation.

To evaluate the potential energy savings associated with the incorporation of olive husk (OH) into concrete, we analyzed the thermal resistance (R) and thermal transmittance (U-value) of the specimens. The thermal resistance was calculated based on the measured thermal conductivity and a standardized wall thickness (0.30 m):

$$R = L/\lambda \quad (6)$$

where R is the thermal resistance ($m^2 \cdot K/W$); L is the wall thickness (m); and λ is the thermal conductivity (W/m·K). The U-value, representing the rate of heat transfer through the material, is the reciprocal of the thermal resistance:

$$U = 1/R \quad (7)$$

The percentage reduction in U-value relative to the control specimen (BLC0) was used to estimate the potential energy savings:

$$\text{Energy saving } (\%) = 100 \times \left(\frac{U_{BLC0} - U_{BLC10,20}}{U_{BLC0}} \right) \quad (8)$$

This approach assumes that reductions in the U-value correlate directly with decreases in heating and cooling energy demands, providing a comparative assessment of the energy efficiency improvements achieved through OH incorporation.

2.2.3. Moisture Buffering Capacity

The moisture buffering performance (MBV) of the materials was evaluated as per a modified NORDTEST protocol [60], as represented in Figure 5. The MBV of a material reflects the ability of hygroscopic materials to absorb and release moisture in response to ambient humidity fluctuations, thereby influencing indoor hygrothermal comfort. Three cylindrical specimens (110 mm in diameter, 20 mm in thickness) were prepared for each formulation. Prior to testing, the specimens were sealed on all but one surface using aluminum tape to ensure unidirectional moisture exchange. The samples were then conditioned to reach equilibrium with ambient air at 21 ± 5 °C and 53 ± 5% relative humidity (RH).

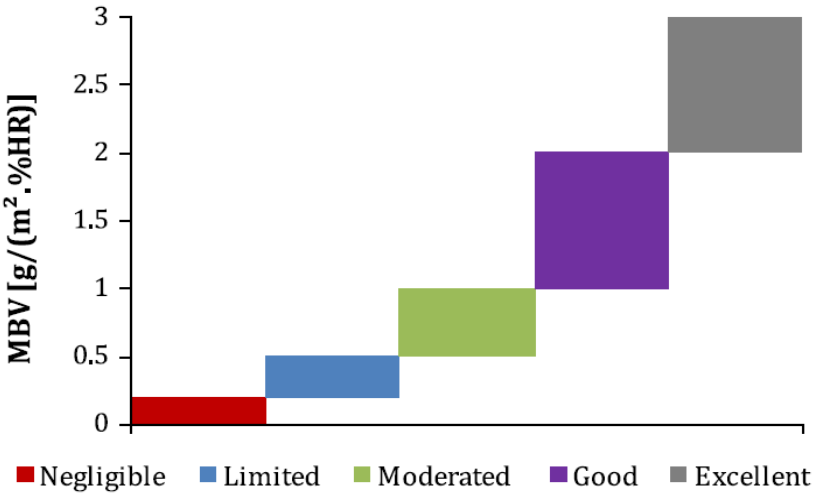

Figure 5. NORDTEST project classification of materials versus moisture buffer value [46].

The specimens were subjected to cyclic humidity variations inside a climatic chamber, where they experienced 8 h at 80% RH followed by 16 h at 40% RH, while the temperature was maintained at 23 °C. The mass variations were recorded with an accuracy of 0.01 g. Once steady-state conditions were achieved, the moisture buffer value (MBV) was calculated using the following equation:

$$\mathrm{MBV} = \frac{\Delta m}{A(RH_{80} - RH_{40})} \quad (9)$$

where (Δm) is the moisture exchanged during one cycle; (A) is the open surface area; and ($RH_{80} - RH_{40}$) is the % RH variation.

2.2.4. Mechanical Properties: Compressive and Flexural Strength

The mechanical performance of the specimens was assessed through flexural and compressive strength tests, following the BS EN 196-1 standard [61]. A PILOT PRO universal testing machine was employed to test prismatic specimens (40 mm × 40 mm × 160 mm), with three replicates prepared for each formulation.

- Flexural strength was determined using a three-point bending test.
- The fractured halves from the bending test were subsequently used for compressive strength evaluation.

2.2.5. X-Ray Diffraction (XRD) and Microstructural Analysis (SEM)

To investigate the crystalline phases, X-ray diffraction (XRD) analysis was performed using a Rigaku SmartLab diffractometer equipped with a copper (Cu) tube. The data were processed using HighScore Plus software v5.3a, employing a search/match algorithm for phase identification, followed by quantitative phase analysis.

The surface morphology and microstructural characteristics of the specimens were analyzed via scanning electron microscopy (SEM). The samples were coated with a thin gold layer prior to imaging to enhance conductivity. The SEM analysis was conducted using a Quanta Inspect S scanning electron microscope, FEI, Holland, MI, USA.

3. Results and Discussion

All tests were conducted on three replicate specimens per formulation (n = 3), and results are reported as mean values. Where applicable, standard deviations were calculated and reported. For calculated properties such as porosity, thermal diffusivity, and effusivity—derived from primary measured values—the variability was considered negligible relative to the measurement error and is therefore not reported as error bars

3.1. Density and Porosity

The incorporation of olive husk (OH) into the bio-based lightweight concrete resulted in a significant reduction in bulk density, decreasing from 2090 kg/m^3 in the control sample (BLC0) to 1653.24 kg/m^3 and 1486.8 kg/m^3 for BLC10 and BLC20, respectively (Table 4). This decrease is attributed to the lower intrinsic density of olive husk compared to conventional mineral aggregates, which effectively reduces the overall mass of the composite. The substitution of sand with olive husk introduces a more porous and less compact matrix, leading to a notable increase in total porosity. Specifically, porosity increased from 20.7% in the control sample to 31.7% and 37.2% in BLC10 and BLC20, respectively. This trend is consistent with the previous studies on bio-based aggregates, where the inclusion of plant-based materials introduces additional voids within the cementitious matrix due to their irregular morphology and higher water absorption capacity.

Table 4. Mean bulk density and total porosity of lightweight concrete as a function of olive husk content (0%, 10%, and 20% by weight), compared with selected lightweight concretes/mortars (n = 3).

Samples ID	Bulk Density (kg/m^3)	True Density (kg/m^3)	Total Porosity (%)	Reference
BCL0	2090	2634.600	20.7	This work
BCL10	1653.24	2421.840	31.7	This work
BCL20	1486.8	2368.350	37.2	This work
Olive pomace 10–15%	1500–1380	-	38–41	[53]
Olive bone-based concrete OP-C10/15%	2013.53/1933.61	-	-	[60]
Vegetable concrete	1060	-	-	[32]
C12/C25	2200	-	-	[32]

The increased porosity is expected to influence the mechanical and hygrothermal performance of the material, as higher porosity typically enhances moisture regulation and thermal insulation properties while potentially reducing mechanical strength. A study by [41] examined the density evolution in mortar mixtures incorporating olive bones, identifying an upper density limit of 2080 kg/m^3 and a lower limit of 1226 kg/m^3, with a stable minimum around 1800 kg/m^3. In a complementary investigation, in [62], it was demonstrated that higher proportions of olive waste impede the formation of essential

hydration products (such as C_3S and C_2S), leading to increased porosity and a consequent reduction in bulk density. Similarly, the research by [56] on the partial replacement of sand with olive bone aggregates in a lightweight mortars at 10%, and 15% levels revealed a systematic rise in porosity of approximately 38%, and 41%, respectively, and a decrease in densities of approximately 1500 and 1380 kg/m^3, respectively. This behavior was mainly attributed to poor adhesion between the aggregates and the cement matrix, coupled with a broader distribution of pores. Further supporting these trends, in a subsequent study [63], the authors reported that the bulk density of olive husk-based concrete (OP-C) decreased systematically with increasing olive husk content, dropping from 2100.47 kg/m^3 at 5% OH to 2013.53 kg/m^3 at 10% and further to 1933.61 kg/m^3 at 15%. A subsequent investigation by the same research group [64] observed similar trends, with densities measured at 2095 kg/m^3 and 2000 kg/m^3 for 10% and 15% doping levels, respectively. Overall, while these investigations provide robust insights into the behavior of olive husk derivatives, particularly olive bones, the literature on raw olive husk remains relatively scarce.

3.2. Thermal Properties

3.2.1. Thermal Conductivity, Specific Heat Capacity, Thermal Diffusivity, Thermal Effusivity, and Thermal Resistance

The thermal conductivity of the bio-based lightweight concrete exhibited a significant reduction with the incorporation of olive husk (Table 5), decreasing from 1.45 W/m·K in the control sample (BLC0) to 0.669 W/m·K and 0.405 W/m·K for BLC10 and BLC20, respectively. This substantial decline can be attributed to the intrinsic low thermal conductivity of olive husk, which effectively disrupts heat transfer pathways within the composite matrix. The increase in total porosity, as previously discussed, further contributes to this reduction by enhancing the presence of air-filled voids, which act as thermal insulators. The progressive decrease in thermal conductivity with higher OH content aligns with prior studies on bio-based aggregates, where plant-derived materials introduce thermal resistance due to their porous structure and organic composition. This reduction in thermal conductivity parallels the broad range of values reported in studies of plant-based aggregates and fibers, where thermal performance is similarly affected by variations in porosity and density [65–69]. Generally, the thermal conductivity increases with the density as reported in [32], where the thermal conductivity of hempcrete varied between 0.06 and 0.19 W/m·K for densities of 200–850 kg/m^3.

Table 5. Mean thermal characteristics of lightweight bio-concrete with 0%, 10%, and 20% olive husk addition (n = 3).

Samples	Bulk Density (kg/m^3)	Thermal Conductivity λ (W/m·K)	Thermal Resistivity R-0.15 m	Specific Heat Capacity Cp (J/kg·K)	Thermal Diffusivity α (m^2/s)	Thermal Effusivity E (J/m^2·s$^{0.5}$·K)
BLC0	2090	1.454 ± 0.025	0.103	1439.44	4.83×10^{-7}	2091.47
BLC10	1653.24	0.669 ± 0.009	0.224	1198.55	3.38×10^{-7}	1151.35
BLC20	1486.8	0.405 ± 0.013	0.370	997.11	2.73×10^{-7}	774.86

The thermal conductivity of bio-based mortars generally declines with increasing plant-based inclusions due to enhanced porosity and reduced bulk density. This trend is well-documented in previous studies. For instance, an investigation into bio-based plasters incorporating olive-tree pruning residues (leaves and small branches) in a clay–sand mixture at 8% and 12% substitution resulted in thermal conductivity values of 0.458 W/(m·K) and 0.428 W/(m·K), respectively [70]. Similarly, a study on lightweight self-compacting mortars (SCLMs) incorporating olive bone shells as a partial sand replacement reported a progressive decrease in thermal conductivity, reaching 0.8 W/(m·K) at 25%

and 50% inclusion and further dropping to 0.294 W/(m·K) at full (100%) substitution [51]. Another study [42] found that adding 10% and 15% olive bones in cement mortar yielded thermal conductivity values of 0.917 W/(m·K) and 0.847 W/(m·K), respectively. Moreover, research on cement–lime mortars incorporating olive bones recorded a significant decline in thermal conductivity from 1.09 W/(m·K) at 0% substitution to 0.63 W/(m·K) at 10%, 0.43 W/(m·K) at 20%, and a minimum of 0.27 W/(m·K) at 70% inclusion [71]. Likewise, the inclusion of 10% and 15% olive waste (OW) in cement-based concrete was found to reduce thermal conductivity to 0.7 W/(m·K) and 0.6 W/(m·K), respectively [48,63].

Furthermore, thermal resistance, which inversely correlates with thermal conductivity, increased substantially as the olive husk content rose. The sample with 20% olive husk (BLC20) exhibited a thermal resistance of 0.740 m^2·K/W (for a 0.3 m thickness), which is over three times that of the control (0.206 m^2·K/W). This enhancement in thermal resistance is particularly advantageous for passive building envelope design, improving insulation and reducing reliance on mechanical heating and cooling systems [20]. These findings closely align with the present study; however, the use of whole olive husk—including pulp, fibers, and bones—introduces additional complexities in thermal behavior. Unlike olive bones alone, the fibrous and porous organic components of whole olive husk contribute to superior insulation properties by reducing thermal conductivity and enhancing moisture buffering capacity, further differentiating its performance from other bio-based aggregates. Notably, the thermal conductivity of both lightweight concrete samples remained below 0.75 W/m·K, meeting the RILEM classification criteria for lightweight aggregate concrete [27], which stipulates a thermal conductivity threshold of 0.75 W/m·K for effective thermal insulation in lightweight concrete. As will further be discussed in the following section, this confirms that OH-based bio-concrete can serve as a viable alternative for applications requiring insulation performance. Additionally, OH bio-composite presents a balanced solution, offering improved structural integrity while maintaining moderate insulation, as will be further examined in the mechanical behavior section.

Figure 6 illustrates the correlation between thermal conductivity and density for the tested samples, alongside comparable materials reported in the literature [14,31,72,73]. The data emphasize that both the binder type and the intrinsic characteristics of bio-aggregates play a crucial role in determining the physical and thermal behavior of lightweight concrete (LWC), in addition to the inclusion percentage. When compared to corn stalk-based concrete [20] and molded hemp concrete at equivalent doping levels, both BLC10 and BLC20 exhibit closer densities—an essential criterion for LWC—while maintaining comparable thermal conductivity values. Moreover, flax shives concrete [14], formulated with a 1:2 fiber-to-binder ratio, demonstrates a thermal performance similar to the tested samples at the same 15% bio-aggregate content.

The thermal behavior of bio-concrete is governed by multiple interconnected parameters beyond thermal conductivity alone, including specific heat capacity, thermal diffusivity, and thermal effusivity. In this study, the incorporation of olive husk significantly influenced these properties. Specific heat capacity, which quantifies a material's ability to store thermal energy, decreased from 1439.44 J/kg·K in the control mix (BLC0) to 997.11 J/kg·K in the BLC20 sample. Despite this reduction, the values remain within the typical range of plant-based concretes, which are reported to exhibit specific heat capacities exceeding those of conventional concrete (typically 800–1200 J/kg·K), with some formulations, such as hemp concrete, reaching up to 1500 J/kg·K in dry conditions and higher under humidity [32].

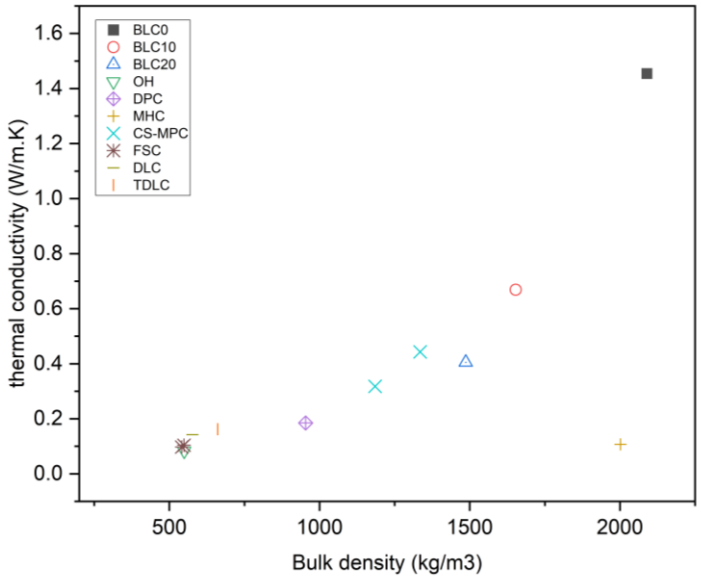

Figure 6. Correlation between thermal conductivity and bulk density for olive husk-modified lightweight concrete (present study) and comparable building materials ([14,31,72,73]), where DPC: date palm concrete; MHC: molded hemp concrete; CS-MPC: corn stalk concrete; FSC: flax shives concrete; DLC: distilled lavender concrete; TDLC: treated distilled lavender concrete.

Thermal diffusivity, which reflects the rate of heat propagation through a material, also showed a decreasing trend—from 4.83×10^{-7} m^2/s for BLC0 to 2.73×10^{-7} m^2/s for BLC20 reaching a low value closer to insulation panels value (1.8×10^{-7} m^2/s) [57]. This reduced diffusivity implies a slower thermal response, beneficial for maintaining the indoor thermal stability and mitigating heat stress, especially in climates with high diurnal temperature variations. These values are in agreement with the literature, where plant-based concretes typically present a lower diffusivity than mineral-based materials, enhancing their thermal damping effect, hempcrete, flax concrete, Typha-clay concrete, and cellular concrete all showed a low thermal diffusivity of 2.6, 2.46, 2.1, and 2.7×10^{-7} m^2/s, respectively [32]. The thermal effusivity of the samples similarly decreased with increasing olive husk content, from 2091.47 $J/m^2 \cdot s^{0.5} \cdot K$ for BLC0 to 774.86 $J/m^2 \cdot s^{0.5} \cdot K$ for BLC20. A low thermal effusivity reduces the rate at which a material exchanges heat with its environment, contributing to a lower sensation of thermal discomfort on contact and improved surface thermal comfort in interior applications [74]. Such behavior is characteristic of bio-aggregates, which are known for their low density and porous structure that suppress both conductivity and effusivity [75].

Collectively, these parameters underscore the importance of considering a composite view of thermal performance in bio-concretes. While thermal conductivity is often the primary metric reported, this study demonstrates that specific heat capacity, thermal diffusivity, and effusivity play critical roles in defining the material's overall thermal behavior. These properties contribute to time lag, energy savings, and improved thermal comfort, reinforcing the suitability of olive husk–based concretes in sustainable construction as will be reported in the next session.

3.2.2. Thermal Time Lag and Energy Savings

For a wall thickness of 0.15 m; consistent with the ASTM C90 Standard Specification for Loadbearing Concrete Masonry Units [76], which recognizes 150 mm as a common thickness for both loadbearing and non-loadbearing applications; the integration of olive husk (OH) into concrete mixtures significantly improved the thermal inertia of the material. This is evidenced by the calculated time lag (φ), which increased from 1.31 h in the control

specimen (BLC0) to 1.87 h in BLC10 and 2.32 h in BLC20 (Figure 7). This improvement is primarily attributed to the substantial reduction in thermal diffusivity, stemming from the lower thermal conductivity and the relatively preserved specific heat capacity introduced by the porous, lignocellulosic nature of the OH. It is worth noting that this thickness represents a conservative configuration, as thicker wall sections would yield even greater time lag values due to the inverse relationship between diffusivity and wall depth. These findings align with previous studies on bio-based materials. For instance, hemp concrete has been reported to exhibit time lag values ranging from 4.2 to 4.6 h for 100 mm thick blocks, largely due to their thermal conductivity, highlighting the potential of plant-based aggregates in enhancing thermal inertia [77]. Similarly, the incorporation of phase change materials with mycelium integration has been shown to delay heat transfer, contributing to improved thermal performance in building envelopes [78].

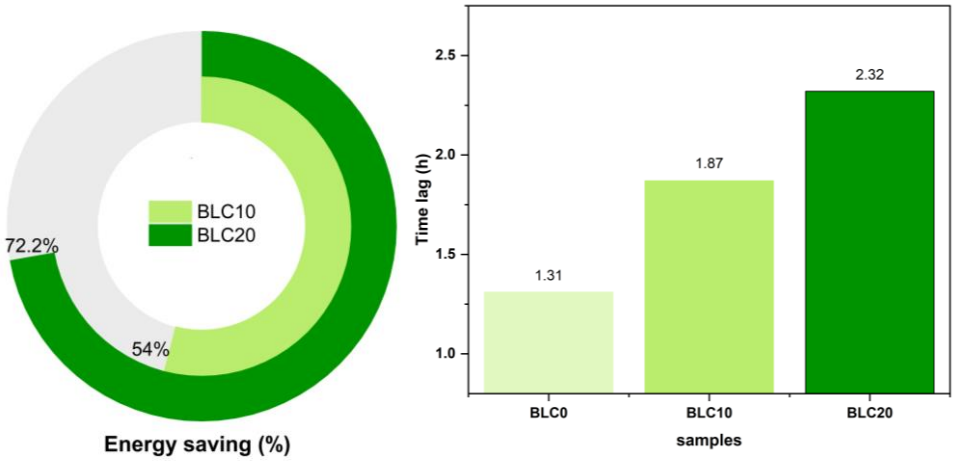

Figure 7. Time lag and energy saving of the olive husk-based bio-lightweight concrete BLC10 and BLC20.

The increased time lag observed in OH-based bio-concrete suggests its efficacy in moderating indoor temperature fluctuations, thereby enhancing occupant comfort and reducing reliance on conventional heating and cooling systems. Thermal resistance (R) also improved considerably. At 0.15 m thickness, the R-value increased from 0.103 m^2·K/W in BLC0 to 0.224 m^2·K/W in BLC10 and 0.370 m^2·K/W in BLC20. Correspondingly, the U-value (thermal transmittance) decreased from 9.709 W/m^2·K to 4.464 W/m^2·K in BLC10 and 2.703 W/m^2·K in BLC20, resulting in projected energy savings of 53.9% and 72.2%, respectively, when compared to the reference concrete. These findings corroborate results from earlier studies, where plant aggregates such as Stipa tenacissima (Alfa fibers) achieved thermal conductivity reductions of over 50%, contributing to energy-efficient building envelopes [79]. Moreover, the enhanced thermal properties of OH-based bio-concrete contribute to the development of energy-efficient building materials. By reducing heat transfer through building envelopes, these materials can play a crucial role in lowering energy demands for indoor climate control, aligning with sustainable construction practices [80].

Although thermal conductivity is widely highlighted as the primary metric in evaluating insulation performance of bio-based lightweight concretes, our findings suggest that it should not be viewed in isolation. Despite the thermal conductivity of our BLC20 specimen (0.405 W/m·K) being slightly higher than values reported for other plant-based concretes such as hempcrete (0.1057 W/m·K) or flax concrete (0.168 W/m·K) and straw rape concrete (0.094 W/m·K) [32], the enhanced thermal performance—reflected in extended time lag and substantial energy savings—is strongly correlated with other thermal parameters, particularly specific heat capacity and volumetric heat storage. For instance, the specific heat capacity of BLC10 (1198.55 J/kg·K) combined with its bulk density (1653 kg/m^3)

yields a volumetric heat capacity of nearly 1.98 MJ/m^3·K, contributing significantly to the material's ability to buffer indoor temperature fluctuations. The increased time lag (1.87 h for BLC10 and 2.32 h for BLC20) delays heat transfer through the wall system, aligning indoor temperature peaks with periods of lower outdoor thermal loads, which enhances indoor thermal comfort and reduces cooling demand.

This synergy between thermal conductivity, specific heat capacity, and time lag underscores that energy-saving potential in bio-concretes arises from the combined effect of all thermal properties, not solely from low λ-values. Therefore, a comprehensive thermal characterization, integrating both steady-state and dynamic parameters, is essential for accurately assessing and optimizing the hygrothermal behavior of plant-based insulating materials.

3.3. Moisture Buffering Capacity (MBV)

The moisture buffering value (MBV) exhibited a significant improvement with the incorporation of olive husk, increasing from 0.21 g/m^2·%RH in the control specimen to 1.22 g/m^2·%RH and 2.18 g/m^2·%RH for the 10% and 20% olive husk-doped samples, respectively (Table 6). According to the NORDTEST classification, these values transition from a "limited" buffering capacity for the control sample to "good" and "excellent" performance for the doped specimens. This enhancement is attributed to the increased porosity and hygroscopic nature of olive husk, which facilitates greater moisture adsorption and desorption cycles. Furthermore, analysis of the final absorption–desorption cycle (Figure 8) reveals that the 20% doped specimen (BLC20) exhibits a steeper slope than BLC10, indicating a more dynamic and efficient moisture exchange process. This suggests that BLC20 is not only capable of storing more moisture but also reacts more responsively to variations in ambient humidity. The enhanced slope reflects a higher rate of moisture uptake and release, which is beneficial for regulating indoor humidity levels in bio-based construction applications.

Table 6. Mean moisture buffer value (MBV), total porosity, and NORDTEST classification of olive husk-modified lightweight concrete composites (n = 3).

Samples ID	Total Porosity n (-)	MBV After 10 Cycles of 24 h (g/m^2 %RH)	NORDTEST Classification [57]
BLC0	0.207	0.21	Limited
BLC10	0.317	1.22	Good
BLC20	0.372	2.18	Excellent

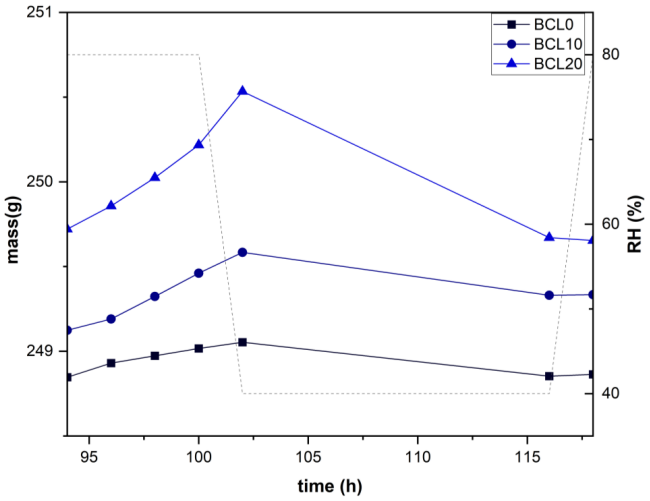

Figure 8. Final absorption–desorption cycle for lightweight concrete with different olive husk contents—mean values from triplicate samples.

The hygric behavior of concrete and mortars incorporating raw olive husk as a bio-aggregate remains underexplored, despite its promising potential in enhancing moisture buffering capacity. However, valuable insights can be drawn from studies examining other olive-derived materials, such as olive tree fibers in unstabilized clayey plasters. A recent study on fiber-reinforced plasters [70], following the NORDTEST protocol, reported ideal moisture buffer values (MBV_ideal) ranging from 1708 to 1739 g/(m^2·%RH) for fiber contents between 4% and 12%, classifying the material as "good" (1 < MBV < 2) [81]. These findings suggest that olive-based materials contribute significantly to improving the hygric performance of mineral-based composites.

Additionally, the research on other bio-based aggregates, such as hemp–clay composites, underscores the pivotal role of bio-aggregates in modifying moisture buffering behavior. For instance, a study investigating flax shives in lime-based concrete demonstrated that increasing the flax shive content led to a substantial enhancement in moisture buffering capacity. Specifically, MBVs rose to 2.18 and 2.45 g/(m^2·%RH) at 11.5% and 14.5% flax shive incorporation, respectively [14]. This trend aligns with the findings of the present study, where the inclusion of olive husk similarly enhanced the MBVs, reinforcing the effectiveness of plant-based additives in improving hygric regulation within mineral-binder matrices. Conversely, the contrast between bio-based and synthetic additives in moisture buffering performance is stark. A study investigating expanded polystyrene-based mortars reported significantly lower MBVs of 0.55 g/(m^2·%RH), while a reference cement paste achieved only 0.8 g/(m^2·%RH) [82]. This disparity highlights the superior hygroscopic properties of bio-aggregates such as hemp, flax, and olive husk, which facilitate a greater moisture exchange with the environment, thereby enhancing indoor hygric stability. Unlike synthetic materials, bio-based aggregates actively interact with ambient humidity, making them promising candidates for sustainable construction materials that contribute to improved indoor air quality and thermal comfort.

3.4. Mechanical Properties

The control sample (BCL0) demonstrated the highest mechanical performance, with compressive and flexural strengths of 36.96 MPa and 8.86 MPa, respectively (Figure 9). This is indicative of a dense, rigid cement matrix characteristic of conventional cement-based materials. In contrast, the incorporation of olive husk significantly reduced both compressive and flexural strengths. Specifically, the sample with 20% olive husk (BLC20) exhibited a compressive strength of 11.68 MPa and a flexural strength of 3.58 MPa, while the 10% olive husk sample (BLC10) showed slightly higher values, with an average compressive strength of 15.21 MPa and a flexural strength of 4.67 MPa. This reduction in mechanical strength is primarily attributable to the increased porosity introduced by the olive husk, which disrupts the continuity of the cementitious matrix. The olive husk, while acting as both a filler and a reinforcing fiber, increases the overall void content within the composite. Although the fibrous component may contribute positively to the interfacial transition zone (ITZ) and slightly mitigate the loss in flexural strength, the dominant effect remains the dilution of the dense cement matrix, leading to lower load-bearing capacity. The observed trend suggests that while a lower dosage (10%) of olive husk may offer a marginal improvement in strength compared to the higher dosage (20%), both doped samples exhibit a significant compromise in mechanical performance relative to the control. This trade-off is acceptable for applications where enhanced thermal and hygrothermal properties are prioritized over structural strength, particularly in non-load-bearing contexts.

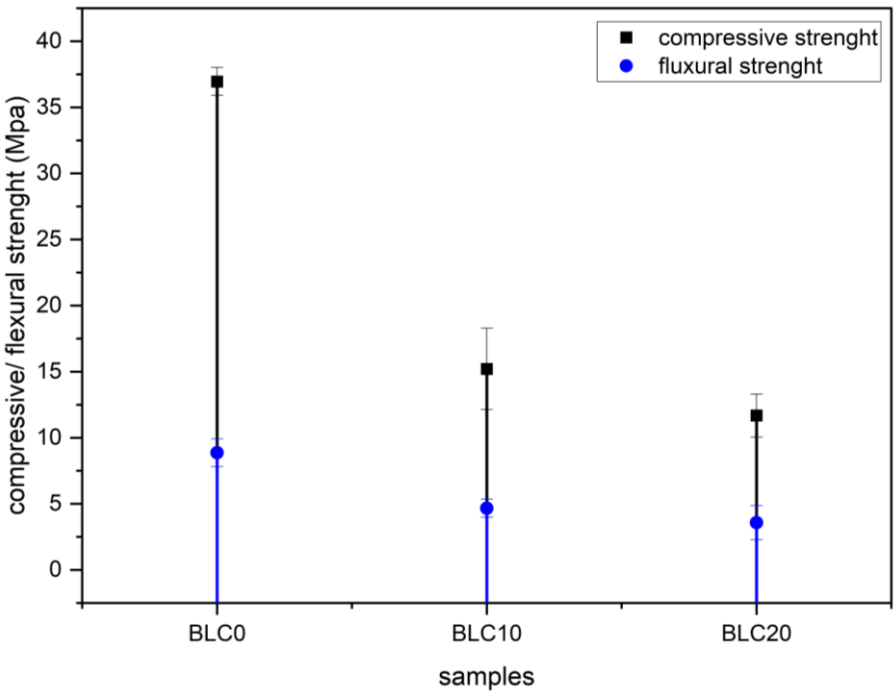

Figure 9. Mechanical properties of BLC0, BLC10, and BLC20: mean compressive and flexural strength values with standard deviations (n = 3).

Several studies have highlighted the trade-offs associated with bio-based aggregates in concrete and mortar, emphasizing the reduction in mechanical strength due to increased porosity and decreased adhesion between the binder and bio-aggregates. A study by El Boukhari et al. [56] reported a significant decline in compressive strength from 40 MPa (control) to approximately 10 MPa and 8 MPa at 10% and 15% bio-aggregate incorporation, where the studied olive husk primarily consisted of olive bones. Similarly, a study on self-compacting lightweight mortar incorporating olive kernel shells (COKs)—a pre-washed form of olive bones—demonstrated a progressive reduction in both compressive and flexural strength as the bio-aggregate content increased [51]. With a binder-to-sand ratio (B/S) of 6.5, the reference mortar (0% COKs) exhibited a compressive strength of 54 MPa, which decreased to 30 MPa at 25% replacement. The flexural strength followed a similar trend, dropping from 8.3 MPa (0% COKs) to 5.2 MPa (25% COKs). These findings highlight the structural trade-offs associated with olive bone incorporation, where the high porosity and low surface adhesion of these particles weaken the mechanical performance of the mortar. In another study, pre-washed and cleaned olive husk—consisting almost exclusively of olive bones—was used as a bio-aggregate, and the results revealed a continuous decline in compressive strength with increasing substitution levels [64]. The strength decreased from approximately 30 MPa at 0% olive husk to 12 MPa at 10% addition and 9 MPa at 15% addition. The mechanical performance was largely affected by the high organic content and residual oils in the olive bones, which hindered cement hydration and bond formation within the matrix. This observation highlights the beneficial effect of the thermal treatment applied to the olive husk in our study.

The boiling process used in our work likely reduced the residual oil content and improved the adhesion between the bio-aggregate and the cementitious matrix, thereby enhancing the overall mechanical performance. This treatment contributed to the higher compressive and flexural strengths observed in our samples compared to those incorporating untreated olive bones. A most recent study specifically investigating the mechanical impact of olive bones on mortar properties [42] found that at 10% and 20% replacement,

the compressive strength reached 10.31 MPa and 9.62 MPa, respectively, while the flexural strength was 2.15 MPa and 1.62 MPa.

In contrast, our results highlight the superior mechanical performance of mortars incorporating whole olive husk, rather than just olive bones. At 10% and 20% olive husk addition, our bio-composites achieved compressive strengths of 15.21 MPa and 11.68 MPa, respectively, while flexural strengths reached 4.67 MPa and 3.58 MPa. These values significantly surpass those obtained with olive bones alone, underscoring the critical role of olive husk fibers in reinforcing the cementitious matrix. The fibrous content enhances tensile resistance, crack-bridging, and overall ductility, mitigating the strength reductions typically observed in bio-based mortars. This distinction demonstrates that while olive bones alone contribute primarily as lightweight fillers, the presence of fibers in whole olive husk offers additional mechanical benefits, particularly in flexural performance. Figure 10 presents typical failure modes after mechanical testing. In (a), the flexural specimen exhibits a clean mid-span crack, indicating brittle fracture. In (b), the compressive specimen shows lateral cracks and surface porosity, suggesting internal weaknesses likely caused by the olive husk inclusion.

Figure 10. Fracture morphology of specimens after mechanical testing: (**a**) compressive failure surfaces; (**b**) flexural failure zones; (**c**) lateral internal view highlighting porosity and material structure.

Studies on olive stone-based mortars further illustrate the impact of cement type on mechanical performance. The research examining different cement strength classes (32.5, 42.5, and 52.5 MPa) with a B/S ratio of 0.2 reported compressive strengths of approximately 9.8 MPa and 9 MPa at 10% and 15% olive stone content with cement 32.5, 11.9 MPa and 11.2 MPa with cement 42.5, and 14 MPa and 13 MPa with cement 52.5, respectively [41]. The study concluded that cement 32.5 significantly compromises the early strength development, making it unsuitable for industrial applications involving high bio-aggregate content. Based on a market viability criterion of 10 MPa at 28 days, cement 42.5 is recommended for mixtures incorporating up to 10% olive stone, while cement 52.5 is necessary for higher doping levels up to 30%. Overall, the mechanical performance of OH-based composites is strongly influenced by both the fibrous content and the cementitious matrix. The presence of fibers in olive husk can enhance crack-bridging effects and tensile resistance but simultaneously introduces weak interfacial zones that compromise compressive strength.

Table 7 presents the functional classification of lightweight concrete (LWC) according to RILEM 1978 [27], which serves as a benchmark for evaluating the thermal and mechanical properties of the BLC10 and BLC20 bio-concretes. The results indicate that both olive husk-based bio-composites meet the criteria for Class II LWC applications, demonstrating their suitability for both insulating and structural purposes. Notably, both compositions fulfil the requirements for Class II LWC, reinforcing their potential as sustainable alternatives for applications requiring a balance of thermal insulation and mechanical performance.

Table 7. Functional classification of bio-based lightweight concrete (BLC10 and BLC20) based on RILEM classification [80].

Types of Concrete				
	*LWC (Rilem [80])		BLC10	BLC20
classification	*Class II	*Class III	Class II	Class II
Compressive strength (Mpa)	>3.5	>0.5	15.21 ± 3.07	11.68 ± 1.63
λ (W/m·K)	<0.75	<0.3	0.669 ± 0.015	0.405 ± 0.020

*LWC = light weight concrete; *Class II = insulating and structural; *Class III = insulating.

3.5. X-Ray Diffraction (XRD)

The XRD analysis was conducted to evaluate the crystalline phases present in both the control and olive husk-doped specimens (BLC10 and BLC20) and to elucidate the impact of OH incorporation on the cementitious matrix, the results are presented in Figure 11. In the control sample, the diffraction patterns revealed distinct peaks corresponding to the conventional hydration products of Portland cement, including portlandite, ettringite, and calcium silicate hydrate (C-S-H) phases. In contrast, the OH-modified samples exhibited notable alterations in their XRD profiles. Specifically, the intensity of the portlandite peaks was markedly reduced in the specimens containing olive husk. This observation suggests that components within the olive husk may participate in a pozzolanic reaction, consuming $Ca(OH)_2$ and promoting the formation of additional C-S-H phases. The transformation of portlandite to C-S-H not only contributes to a denser microstructure but may also enhance the binding properties of the matrix, thereby positively influencing the mechanical performance. Furthermore, minor shifts in peak positions and changes in relative intensities were observed in the OH-doped samples. These modifications are likely associated with the incorporation of organic constituents from the olive husk and the resultant alteration of the microstructural environment. The dual functionality of olive husk—as both a fiber and an aggregate—appears to induce a more interconnected and refined microstructure.

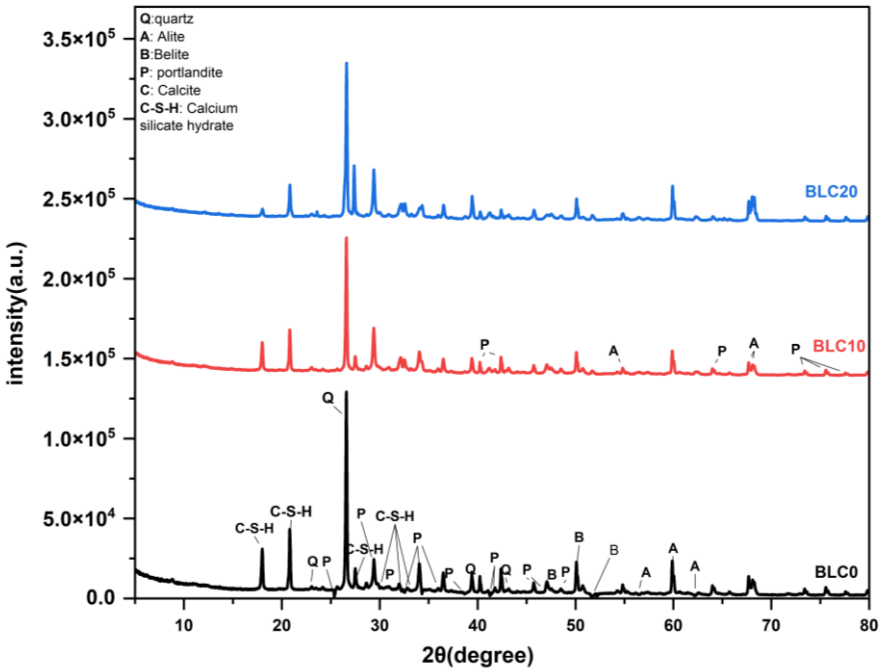

Figure 11. X-ray diffraction (XRD) patterns of lightweight concrete samples: control, 10% olive husk (BLC10), and 20% olive husk (BLC20).

This improved microstructural arrangement is consistent with the enhancements observed in both the thermal and hygrothermal properties of the bio-based concrete. Incor-

porating plant-based materials into cementitious composites can influence the hydration process due to the presence of organic compounds such as sugars, hemicellulose, and lignin, which are known to retard cement hydration and prolong the setting time [83]. A study on the incorporation of distilled lavender stalks in cementitious binders [73] reported a noticeable reduction in calcium hydroxide (C-H) content, as well as a decline in the intensity of XRD peaks associated with cement hydration phases, indicating a diminished degree of hydration. Similarly, research on banana fiber-reinforced concrete [84] observed a decrease in the intensity of hydration-related crystalline phases, suggesting an alteration in the cement matrix's microstructure, particularly at fiber dosages exceeding 2%. Although quantitative peak intensity ratios or area integration were not carried out, the relative decrease in portlandite peak intensity in the OH-incorporated composites provides qualitative evidence of pozzolanic reactivity and secondary C-S-H formation.

3.6. Microstructural Analysis (SEM)

Scanning electron microscopy (SEM) provided valuable microstructural insights into both the raw olive husk (OH) and the impact of its incorporation on the cementitious matrix within OH-doped mortars. SEM micrographs of the olive husk itself revealed a complex microstructure, characterized by a prominent, interconnected network of cellulosic fibers interspersed with finer, amorphous particulate matter. This dual morphology suggests the potential for OH to function both as a reinforcing agent, due to its fibrous structure, and as an inert filler, contributing to improved packing density within the cement matrix. In the doped mortar specimens (LOH10 and LOH20), SEM analysis indicated a relatively uniform distribution of OH particles throughout the cement paste. While primarily acting as a filler material, the inclusion of OH resulted in a more heterogeneous microstructure compared to the control sample [mention the control sample, and its name]. This heterogeneity contributes to increased overall porosity within the mortar, a characteristic known to enhance thermal insulation and moisture buffering capacity as already reported in Sections 2 and 3. However, the increased porosity was more pronounced in the LOH20 samples.

Moreover, in this study, the interfacial transition zone (ITZ) was examined and visualized using scanning electron microscopy (SEM) for both samples (Figure 12), the SEM analysis highlights a refined interfacial transition zone (ITZ) between the cement matrix and the olive husk particles. The enhanced surface roughness of the thermally pre-treated OH promotes superior mechanical interlocking, leading to a more cohesive ITZ with fewer microcracks or debonded regions. Notably, the maintained integrity of the ITZ in the LOH20 sample, despite the higher OH content, suggests that the thermal pre-treatment effectively mitigated any potential weakening effects associated with increased organic matter within the cement matrix. This indicates that the treatment not only allows for increased porosity—beneficial for hygrothermal properties—but also maintains the structural integrity of the composite by preserving a strong and durable ITZ. This dual functionality of olive husk—acting as both a filler and a reinforcing agent—plays a pivotal role in balancing the material's hygrothermal properties with its mechanical performance. The observed characteristics of the interfacial transition zone (ITZ) in our OH-doped mortars are consistent with the findings from previous studies employing various agricultural by-products in cementitious composites. Specifically, a study on self-compacting lightweight mortar containing olive kernel shells (COKs) [51] as aggregate reported a good adhesion between the cement matrix and the COK particles, yet they reported a vacuum creation within the ITZ. Another study by [63] reported that olive bones, when used as a filler in vegetal concrete, exhibited minimal chemical reactivity with cement hydrates, leading to the formation of distinct ITZs between the olive bones and the cement matrix. This observation aligns with our findings, where the thermally treated OH (boiled OH) appeared to

primarily act as a filler, although with enhanced mechanical interlocking due to the surface roughness imparted by the thermal pre-treatment. In contrast, a separate study by our research group (under review) revealed significantly weaker adhesion between untreated olive husk particles and the cement matrix in cement mortar composites. Similarly, in rice husk concrete, the formation of weak ITZ zones was reported, which are more prone to crack development [85]. These ITZ zones, characterized by poor bonding between the bio-based filler and the cementitious binder, highlight the challenges associated with the incorporation of organic fillers in cementitious materials. It is noteworthy that numerous researchers have explored modification techniques to improve the performance of these bio-based materials in cementitious composites and address the challenges associated with weak ITZs. A study by Faso, B. [86], for instance, examined the effects of various treatments on oil palm shell (OPS) aggregates, including lime treatment, sodium silicate (SS) treatment, polyvinyl alcohol (PVA) treatment, heat treatment (HT), and pre-wetting treatment. Their results indicated that lime treatment of OPS aggregates prior to incorporation into the cementitious material enhanced adhesion between the cement paste and the OPS particles, resulting in an approximately 10% improvement in compressive strength after 28 days. Another study [87] also highlight the importance of surface modification techniques to enhance the compatibility between natural fibers and the cement matrix. The thermal pre-treatment employed in our study represents a similar approach for improving the properties of the OH and promoting a more durable and robust ITZ, thereby addressing the limitations associated with using untreated organic fillers.

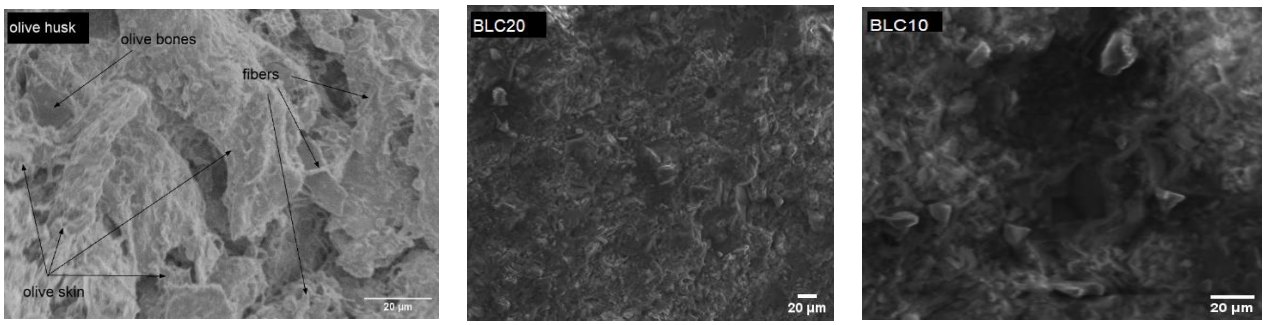

Figure 12. Scanning electron microscopy (SEM) micrographs of olive husk and olive husk-reinforced lightweight concrete BLC10 and BLC20.

4. Conclusions

This study explores the integration of thermally treated olive husk (OH) as a sustainable, bio-based additive for lightweight concrete, with the aim of enhancing its thermal, hygric, and mechanical performance. Using OH in its unfractionated form at substitution levels of 10% and 20% by volume of aggregates, this research evaluates its influence on the composite's physical structure, thermal behavior, moisture buffering capacity, mechanical strength, and microstructural characteristics. The objective is to assess OH's viability as a renewable material for the formulation of low-impact, thermally efficient concretes suited for energy-conscious building applications and offering a comprehensive characterization of thermal behavior, which extends beyond thermal conductivity—a limitation commonly identified in the existing literature. By incorporating specific heat capacity, thermal diffusivity, thermal effusivity, time lag, and estimated energy savings, this work delivers a complete thermal profile of bio-based concrete. This level of detail is rarely found in previous studies and offers new insights into how plant-based aggregates affect not just insulation capacity but the entire thermal response of cementitious systems.

- The inclusion of OH significantly altered the internal structure of the concrete matrix. At 20% substitution, bulk density decreased from 2090 to 1486.8 kg/m^3 (–29%), while

total porosity increased, reflecting the porous and low-density nature of the bio-aggregate. This density reduction directly contributes to weight savings in structural applications and aligns with the classification of lightweight concrete, while increased porosity facilitates enhanced hygric and thermal interaction with the environment.

- Thermal conductivity exhibited a marked reduction from 1.454 to 0.405 W/(m·K) with 20% OH addition—a 72% decrease. This was accompanied by an increase in specific heat capacity and a significant decrease in thermal diffusivity (from 4.83×10^{-7} to 2.73×10^{-7} m^2/s). These results underscore the improved thermal insulation potential of OH-based concretes and demonstrate their capacity to delay and buffer temperature transmission through building components.
- For a standardized wall thickness of 0.15 m, the time lag increased from 1.31 to 2.32 h with 20% OH incorporation, enhancing the thermal inertia of the concrete by 77%. This improvement corresponds to a notable increase in thermal resistance (from 0.103 to 0.370 $m^2 \cdot K/W$) and a 72% reduction in the U-value. Such enhancement in thermal delay and resistance supports the suitability of OH-based concrete in passive building strategies, especially in climates with large diurnal thermal variations.
- Moisture Buffer Value (MBV) measurements confirmed a transition from "Limited" (0.21 $g/(m^2 \cdot \%RH)$) in the control to "Excellent" (2.18 $g/(m^2 \cdot \%RH)$) classification in BLC20. This dramatic improvement suggests strong potential for regulating indoor humidity, improving occupant comfort, and reducing reliance on active HVAC systems.
- Despite increased porosity, mechanical strength remained within acceptable limits for non-structural applications. The compressive strength of BLC20 reached 11.68 MPa, with a flexural strength of 3.58 MPa. The fibrous structure of OH contributed to improved ductility and crack-bridging effects, partially compensating for strength losses due to increased porosity. These results reflect a favorable balance between thermal/hygric benefits and mechanical integrity.
- SEM images and XRD analysis revealed a denser matrix with improved particle–matrix adhesion in the OH-modified concretes. Thermal treatment of OH not only removed residual oils, enhancing adhesion, but also contributed to a much more maintained C–S–H formation and reduced portlandite content. This suggests an additional chemical benefit from OH incorporation, promoting long-term microstructural stability.
- Based on RILEM recommendations, BLC10 and BLC20 both fall under Class II of lightweight concretes for non-loadbearing and insulating applications. This classification confirms the practical viability of these formulations in sustainable building contexts, especially where thermal and hygric regulation is prioritized.

This study confirms that olive husk can serve as a multifunctional bio-additive in concrete, offering a synergistic enhancement of thermal insulation, moisture buffering, and mechanical characteristics while significantly lowering density and enhancing the porosity. The composite's performance qualifies it for energy-efficient, non-structural applications such as partition walls or infill panels. Nonetheless, several limitations must be addressed in future work. These include durability under real environmental stressors (e.g., freeze–thaw, wet–dry, biological degradation), long-term mechanical stability, and fire resistance. Additionally, exploring compatibility with alternative low-carbon binders and investigating scalability in pilot constructions will be essential to advance the industrial applicability of this promising bio-based material.

Author Contributions: Conceptualization, H.B. and A.B.; methodology, H.B. and A.B.; validation, H.B, N.B., and A.B.; formal analysis, H.B., N.B., and A.B.; investigation, H.B., N.B., and A.B.; resources, H.B., N.B., and A.B.; data curation, H.B., N.B., and A.B.; writing—original draft preparation, H.B.,

N.B., and A.B.; writing—review and editing, H.B., N.B., and A.B.; visualization, H.B., N.B., and A.B.; supervision, N.B. and A.B.; project administration, A.B.; funding acquisition, H.B., N.B., and A.B. All authors have read and agreed to the published version of the manuscript.

Funding: This research received no external fund.

Data Availability Statement: Data available on request from the corresponding authors.

Acknowledgments: The first author gratefully acknowledges Liverpool John Moores University (LJMU) and the BEST Research Institute for providing the facilities for experimental work. She also express her sincere gratitude Khemissi Belhadad for his invaluable logistical, material, and support throughout the research.

Conflicts of Interest: The authors declare no conflicts of interest.

References

1. Fennell, P.S.; Davis, S.J.; Mohammed, A. Decarbonizing cement production. *Joule* **2021**, *5*, 1305–1311. [CrossRef]
2. Farhadi, F. Carbon Footprint in Construction; Ultimate Guide in 2024. Available online: https://neuroject.com/carbon-footprint-in-construction/ (accessed on 5 January 2024).
3. 2021 Global Status Report 2021 Global Status Report. 2021. Available online: https://globalabc.org/sites/default/files/2021-10/GABC_Buildings-GSR-2021_BOOK.pdf (accessed on 3 March 2025).
4. Available online: https://www.specifyconcrete.org/blog/what-exactly-is-lightweight-concrete (accessed on 3 March 2025).
5. Elango, K.S.; Sanfeer, J.; Gopi, R.; Shalini, A.; Saravanakumar, R.; Prabhu, L. Properties of light weight concrete—A state of the art review Materials Today: Proceedings Properties of light weight concrete—A state of the art review. *Mater. Today Proc.* **2021**, *46*, 4059–4062. [CrossRef]
6. Kubba, S. Green Building Materials and Products. In *Handbook of Green Building Design and Construction*; LEED, BREEAM, and Green Globes; Butterworth-Heinemann: Oxford, UK, 2017; pp. 257–351. [CrossRef]
7. Alharthai, M.; Ozkilic, Y.O.; Karalar, M.; Mydin, M.A.O.; Ozdoner, N.; Celik, A.I. Performance of aerated lightweighted concrete using aluminum lathe and pumice under elevated temperature. *Steel Compos. Struct.* **2024**, *51*, 271–288. [CrossRef]
8. Bumanis, G.; Vitola, L.; Pundiene, I.; Sinka, M. Gypsum, Geopolymers, and Starc—Alternative Binders for Bio-Based Building Materials: A Review and Life-Cycle Assessment. *Sustainability* **2020**, *12*, 5666. [CrossRef]
9. Lelievre, D.; Colinart, T.; Glouannec, P. Hygrothermal behavior of bio-based building materials including hysteresis effects: Experimental and numerical analyses. *Energy Build.* **2014**, *84*, 617–627. [CrossRef]
10. Associada, P. Moisture Buffering Capacity of Earth Mortar Plasters and Hemp Concrete Effect of Temperature and Thickness. Master's Thesis, Universidade NOVA de Lisboa, Lisboa, Portugal, 2015.
11. Kingsley, E.; Calabria-holley, J.; Paine, K. Industrial Crops & Products Physico-mechanical and morphological behavior of hydrothermally treated plant fibers in cementitious composites. *Ind. Crops Prod.* **2023**, *200*, 116832. [CrossRef]
12. Picandet, V. Characterization of Plant-Based Aggregates. In *Bio-Aggregate-Based Building Materials*; Amziane, S., Arnaud, L., Challamel, N., Eds.; Wiley: Hoboken, NJ, USA, 2013. [CrossRef]
13. Lagouin, M.; Laborel-Préneron, A.; Magniont, C.; Geoffroy, S.; Aubert, J.E. Effects of organic admixtures on the fresh and mechanical properties of earth-based plasters. *J. Build. Eng.* **2021**, *41*, 102379. [CrossRef]
14. Benmahiddine, F.; Cherif, R.; Bennai, F.; Belarbi, R.; Tahakourt, A.; Abahri, K. Effect of flax shives content and size on the hygrothermal and mechanical properties of flax concrete. *Constr. Build. Mater.* **2020**, *262*, 120077. [CrossRef]
15. Labat, M.; Magniont, C.; Oudhof, N.; Aubert, J.E. From the experimental characterization of the hygrothermal properties of straw-clay mixtures to the numerical assessment of their buffering potential. *Build. Environ.* **2016**, *97*, 69–81. [CrossRef]
16. Palumbo, M.; Lacasta, A.M.; Holcroft, N.; Shea, A.; Walker, P. Determination of hygrothermal parameters of experimental and commercial bio-based insulation materials. *Constr. Build. Mater.* **2016**, *124*, 269–275. [CrossRef]
17. Vega, P.; Juan, A.; Ignacio Guerra, M.; Morán, J.M.; Aguado, P.J.; Llamas, B. Mechanical characterisation of traditional adobes from the north of Spain. *Constr. Build. Mater.* **2011**, *25*, 3020–3023. [CrossRef]
18. Braiek, A.; Karkri, M.; Adili, A.; Ibos, L.; Ben Nasrallah, S. Estimation of the thermophysical properties of date palm fibers/gypsum composite for use as insulating materials in building. *Energy Build.* **2017**, *140*, 268–279. [CrossRef]
19. Bellel, N.; Boufendi, T. Characterization of biosourced materials cement- date palm fibers. *J. New Technol. Mater.* **2020**, *10*, 26–30. [CrossRef]
20. Chikhi, M. Young's modulus and thermophysical performances of bio-sourced materials based on date palm fibers. *Energy Build.* **2016**, *129*, 589–597. [CrossRef]
21. Rasoul, Z.S.; Juoi, J.M.; Mohamad, M.; Fawzi, N.M. Date palm fiber(DPF) and its composites: A comprehensive survey. *Int. J. Adv. Sci. Technol.* **2020**, *29*, 1776–1788.

22. Ali, A.; Dadi, A.; Ban-Nah, A. Measurement of the Thermal Conductivities of Clay Materials Stabilized by a Mixed Binder. *Phys. Sci. Int. J.* **2023**, *27*, 1–8. [CrossRef]
23. Cintura, E.; Nunes, L.; Faria, P. Characterization of agro-wastes to be used as aggregates for eco-efficient insulation boards. In Proceedings of the International Conference Construction, Energy Environment & Sustainability, Coimbra, Portugal, 12–15 October 2021.
24. Ali, A.; Benelmir, R.; Tanguier, J.-L.; Saleh, A. Caractéristiques mécaniques de l'argile de Ndjamena stabilisée par la gomme arabique. *Afrique Sci.* **2017**, *13*, 330–341.
25. Wang, S.; Li, H.; Zou, S.; Zhang, G. Experimental research on a feasible rice husk/geopolymer foam building insulation material. *Energy Build.* **2020**, *226*, 110358. [CrossRef]
26. Heniegal, A.M.; Ramadan, M.A.; Naguib, A.; Agwa, I.S. Study on properties of clay brick incorporating sludge of water treatment plant and agriculture waste. *Case Stud. Constr. Mater.* **2020**, *13*, e00397. [CrossRef]
27. RILEM. Functional classification of lightweight concretes. *Mater. Struct.* **1978**, *11*, 281–282.
28. Collet, F.; Pretot, S. Experimental investigation of moisture buffering capacity of sprayed hemp concrete. *Constr. Build. Mater.* **2012**, *36*, 58–65. [CrossRef]
29. McGregor, F.; Heath, A.; Fodde, E.; Shea, A. Conditions affecting the moisture buffering measurement performed on compressed earth blocks. *Build. Environ.* **2014**, *75*, 11–18. [CrossRef]
30. Roels, S.; Carmeliet, J. Water vapour permeability and sorption isotherm of coated gypsum board. In Proceedings of the 7th Sumposium on Building Physics in the Nordic Countries, Reykjavik, Iceland, 13–15 June 2014.
31. Chennouf, N.; Agoudjil, B.; Alioua, T.; Boudenne, A.; Benzarti, K. Experimental investigation on hygrothermal performance of a bio-based wall made of cement mortar filled with date palm fibers. *Energy Build.* **2019**, *202*, 109413. [CrossRef]
32. Bakkour, A.; Ouldboukhitine, S.E.; Biwole, P.; Amziane, S. A review of multi-scale hygrothermal characteristics of plant-based building materials. *Constr. Build. Mater.* **2024**, *412*, 134850. [CrossRef]
33. Medouni-Haroune, L.; Zaidi, F.; Medouni-Adrar, S.; Kecha, M. Olive Pomace: From an Olive Mill Waste to a Resource, an Overview of the New Treatments. *J. Crit. Rev.* **2018**, *5*, 1–6. [CrossRef]
34. Edition, E. International Olive Council Newsletter N°187. 2023. Available online: https://www.internationaloliveoil.org/wp-content/uploads/2023/12/NEWSLETTER-187-ENG.pdf (accessed on 5 January 2024).
35. Stones, O.; Francisco, J.; Cuevas, M.; Feng, C.; Mateos, P.Á.; Torres, M. Energetic Valorisation of Olive Biomass: Olive-Tree pruning, olive stones and pomaces. *Processes* **2020**, *8*, 511. [CrossRef]
36. Cintura, E.; Nunes, L.; Esteves, B.; Faria, P. Agro-industrial wastes as building insulation materials: A review and challenges for Euro-Mediterranean countries. *Ind. Crops Prod.* **2021**, *171*, 113833. [CrossRef]
37. Enaime, G.; Dababat, S.; Wichern, M.; Lübken, M. Olive mill wastes: From wastes to resources. *Environ. Sci. Pollut. Res.* **2024**, *31*, 20853–20880. [CrossRef]
38. Moreno-maroto, M.; Uceda-rodríguez, M.; Cobo-ceacero, C.J.; Hoces, D.; Angeles, M.; Martínez, C.; Ana, B.L. Recycling of 'alperujo' (olive pomace) as a key component in the sintering of lightweight aggregates. *J. Clean. Prod.* **2019**, *239*, 118041. [CrossRef]
39. Sansoucy, R. Problèmes généraux de l'utilisation des sous-produits agro-industriels en alimentation animale dans la région méditerranéenne. *Option Méditerranéenne Séries Séminaires* **1991**, *16*, 75–79.
40. Kuruc, M.; Štefunková, Z. Properties of Olive Stones with a View to Their use as Lightweight Aggregate in Construction Mortars. *Slovak J. Civ. Eng.* **2024**, *32*, 52–57. [CrossRef]
41. Ferreiro-Cabello, J.; Fraile-Garcia, E.; Pernia-Espinoza, A.; Martinez-de-Pison, F.J. Strength Performance of Different Mortars Doped Using Olive Stones as Lightweight Aggregate. *Buildings* **2022**, *12*, 1668. [CrossRef]
42. Vicente-Navarro, A.S.; Ferreiro-Cabello, J.; Santos-Ortega, J.L.; Fraile-Garc, E. Methodology for Sustainability Assessment for the Use of Ground Olive Stones in Mortar Bricks for Facades. *Appl. Sci.* **2024**, *14*, 3388. [CrossRef]
43. La Rubia-García, M.D.; Yebra-Rodríguez, Á.; Eliche-Quesada, D.; Corpas-Iglesias, F.A.; López-Galindo, A. Assessment of olive mill solid residue (pomace) as an additive in lightweight brick production. *Constr. Build. Mater.* **2012**, *36*, 495–500. [CrossRef]
44. Christoforou, E.A.; Fokaides, P.A. Thermochemical Properties of Pellets Derived from Agro-residues and the Wood Industry. *Waste Biomass Valorization* **2017**, *8*, 1325–1330. [CrossRef]
45. De La Casa, J.A.; Castro, E. Recycling of washed olive pomace ash for fired clay brick manufacturing. *Constr. Build. Mater.* **2014**, *61*, 320–326. [CrossRef]
46. Eliche-Quesada, D.; Felipe-Sesé, M.A.; Infantes-Molina, A. Olive Stone Ash as Secondary Raw Material for Fired Clay Bricks. *Adv. Mater. Sci. Eng.* **2016**, *2016*, 8219437. [CrossRef]
47. Tayeh, B.A.; Nyarko, M.H.; Zeyad, A.M.; Harazin, S.Z. Al Properties and durability of concrete with olive waste ash as a partial cement replacement Properties and durability of concrete with olive waste ash as a partial cement replacement. *Adv. Concr. Constr.* **2021**, *11*, 59–71. [CrossRef]

48. El, M.; Merroun, O.; Maalouf, C.; Bogard, F. Enhancing mechanical and thermal properties of sustainable cement mortar through incorporation of olive solid waste aggregates Materials Today: Proceedings Enhancing mechanical and thermal properties of sustainable cement mortar through incorporation of olive solid waste aggregates. *Mater. Today Proc.* **2023**, *in press*. [CrossRef]
49. Merino, R.; Rodríguez, G.; Martínez, F.; Astorqui, C.; Santa, J.; Rodríguez, J.G.; Martínez, F.F. Viability of using olive stones as lightweight aggregate in construction mortars Viabilidad del uso de huesos de aceituna como agregado ligero en morteros para la construcción. *Rev. Construcción* **2017**, *16*, 431–438. [CrossRef]
50. Lila, K.; Belaadi, S.; Solimando, R.; Ralida, F. Valorisation of organic waste: Use of olive kernels and pomace for cement manufacture. *J. Clean. Prod.* **2020**, *277*, 123703. [CrossRef]
51. Cheboub, T.; Senhadji, Y.; Khelafi, H.; Escadeillas, G. Investigation of the engineering properties of environmentally-friendly self-compacting lightweight mortar containing olive kernel shells as aggregate. *J. Clean. Prod.* **2019**, *249*, 119406. [CrossRef]
52. Barclay, M.; Holcroft, N.; Shea, A.D. Methods to determine whole building hygrothermal performance of hemp-lime buildings. *Build. Environ.* **2014**, *80*, 204–212. [CrossRef]
53. Almabrok, M.H.; Mclaughlan, R.G.; Vessalas, K.; Thomas, P. Effect of oil contaminated aggregates on cement hydration American Journal of Engineering Research (AJER) Effect of oil contaminated aggregates on cement hydration. *Am. J. Eng. Res.* **2019**, *8*, 81–89.
54. Kazemi, F.; Shafighfard, T.; Yoo, D. Data-Driven Modeling of Mechanical Properties of Fiber-Reinforced Concrete: A Critical Review. *Arch. Comput. Methods Eng.* **2024**, *31*, 2049–2078. [CrossRef]
55. Soudani, L.; Fabbri, A.; Mcgregor, F. Laboratory investigation of hygrothermal monitoring of hemp- concrete walls. *RILEM Tech. Lett.* **2017**, *2*, 20–26. [CrossRef]
56. EL Boukhari, M.; Merroun, O.; Maalouf, C.; Bogard, F.; Kissi, B. Mechanical performance of cement mortar with olive pomace aggregates and olive mill wastewater: An experimental investigation. *Cogent Eng.* **2023**, *10*, 2212522. [CrossRef]
57. Liuzzi, S.; Rubino, C.; Stefanizzi, P.; Martellotta, F. Performance characterization of broad band sustainable sound absorbers made of almond skins. *Materials* **2020**, *13*, 5474. [CrossRef]
58. *ASTM D4892-14*; Standard Test Method for Density of Solid Pitch (Helium Pycnometer Method). ASTM International: West Conshohocken, PA, USA, 2014.
59. *ISO 9869-1:2014*; Thermal Insulation—Building Elements—In-Situ Measurement of Thermal Resistance and Thermal Transmittance—Part 1: Heat Flow Meter Method. International Organization for Standardization (ISO): Geneva, Switzerland, 2014.
60. Rode, C.; Peuhkuri, R.H.; Hansen, K.K.; Time, B.; Svennberg, K.; Arfvidsson, J.; Ojanen, T. NORDTEST Project on Moisture Buffer Value of Materials. In *AIVC 26th Conference: Ventilation in Relation to the Energy Performance of Buildings*; Air Infiltration and Ventilation; INIVE eeig: Amsterdam, The Netherlands, 2005; pp. 47–52.
61. *BS EN 196-1*; Methods of Testing Cement. Determination of Strength. British Standards Institution (BSI): London, UK, 2016.
62. Alkheder, S.; Obaidat, Y.T.; Taamneh, M. Effect of olive waste (Husk) on behavior of cement paste. *Case Stud. Constr. Mater.* **2016**, *5*, 19–25. [CrossRef]
63. El, M.; Merroun, O.; Maalouf, C.; Bogard, F. Exploring the impact of partial sand replacement with olive waste on mechanical and thermal properties of sustainable concrete. *Clean. Mater.* **2023**, *9*, 100202. [CrossRef]
64. El, M.; Merroun, O.; Maalouf, C.; Bogard, F.; Kissi, B. Experimental investigation on the mechanical strength and thermal conductivity of concrete lightened by olive mill solid waste Materials Today: Proceedings Experimental investigation on the mechanical strength and thermal conductivity of concrete lighten. *Mater. Today Proc.* 2023, *in press*. [CrossRef]
65. Benaniba, S.; Driss, Z.; Djendel, M.; Raouache, E.; Boubaaya, R. Thermo-mechanical characterization of a bio-composite mortar reinforced with date palm fiber. *J. Eng. Fibers Fabr.* **2020**, *15*, 1–9. [CrossRef]
66. Latapie, S.R.; Sabathier, V. Bio-based building materials: A prediction of insulating properties for a wide range of agricultural by-products Bio-based building materials: A prediction of insulating properties for a wide range of agricultural by-products. *J. Build. Eng.* **2024**, *86*, 108867. [CrossRef]
67. Nasr, Y.; El Zakhem, H.; Hamami, A.E.A.; El Bachawati, M.; Belarbi, R. Comprehensive Review of Innovative Materials for Sustainable Buildings' Energy Performance. *Energies* **2025**, *16*, 7440. [CrossRef]
68. Brouard, Y.; Belayachi, N.; Hoxha, D.; Ranganathan, N.; Méo, S. Mechanical and hygrothermal behavior of clay—Sunflower (Helianthus annuus) and rape straw (Brassica napus) plaster bio-composites for building insulation. *Constr. Build. Mater.* **2018**, *161*, 196–207. [CrossRef]
69. Vicente-navarro, A.S.; Mend, M.; Santos-ortega, J.L. Alternative Use of the Waste from Ground Olive Stones in Doping Mortar Bricks for Sustainable Façades. *Buildings* **2023**, *13*, 2992. [CrossRef]
70. Liuzzi, S.; Rubino, C.; Stefanizzi, P.; Petrella, A.; Boghetich, A.; Casavola, C.; Pappalettera, G. Hygrothermal properties of clayey plasters with olive fibers. *Constr. Build. Mater.* **2018**, *158*, 24–32. [CrossRef]
71. Barreca, F.; Fichera, C.R. Use of olive stone as an additive in cement lime mortar to improve thermal insulation. *Energy Build.* **2013**, *62*, 507–513. [CrossRef]

72. Ahmad, M.R.; Chen, B.; Yousefi Oderji, S.; Mohsan, M. Development of a new bio-composite for building insulation and structural purpose using corn stalk and magnesium phosphate cement. *Energy Build.* **2018**, *173*, 719–733. [CrossRef]
73. Ratiarisoa, R.V.; Magniont, C.; Ginestet, S.; Oms, C.; Escadeillas, G. Assessment of distilled lavender stalks as bioaggregate for building materials: Hygrothermal properties, mechanical performance and chemical interactions with mineral pozzolanic binder. *Constr. Build. Mater.* **2016**, *124*, 801–815. [CrossRef]
74. Lamrani, M.; Laaroussi, N.; Khabbazi, A.; Khalfaoui, M.; Garoum, M.; Feiz, A. Experimental study of thermal properties of a new ecological building material based on peanut shells and plaster. *Case Stud. Constr. Mater.* **2017**, *7*, 294–304. [CrossRef]
75. Cagnon, H.; Aubert, J.E.; Coutand, M.; Magniont, C. Hygrothermal properties of earth bricks. *Energy Build.* **2014**, *80*, 208–217. [CrossRef]
76. *ASTM C90-22a*; ASTM International Standard Specification for Loadbearing Concrete Masonry Units. ASTM: West Conshohocken, PA, USA, 2022.
77. Rahim, M.; Douzane, O.; Tran Le, A.D.; Langlet, T. Effect of moisture and temperature on thermal properties of three bio-based materials. *Constr. Build. Mater.* **2016**, *111*, 119–127. [CrossRef]
78. Swiety, D. Comprehensive Evaluation of Thermal Performance and Time-Lag in Residential Apartments: A Numerical Simulation Study on Phase Change Material with Mycelium Integration in Amman. In Proceedings of the EnSci Paris 2024–International Conference on Engineering & Sciences, Paris, France, 12–13 January 2024; Proceedings of Scientific and Technical Research Association (STRA). pp. 2–3.
79. Necib, H.; Belatrache, D.; Goutar, H.; Sahraoui, N. Experimental study of thermal conductivity of concrete with biosourced material for saved energy. *Ann. West Univ. Timisoara. Phys. Ser.* **2022**, *64*, 158–171. [CrossRef]
80. Lee, Y.H.; Chua, N.; Amran, M.; Lee, Y.Y.; Kueh, A.H.; Fediuk, R.; Vatin, N.; Vasilev, Y. Thermal Performance of Structural Lightweight Concrete Composites for Potential Energy Saving. *Crystals* **2021**, *11*, 461. [CrossRef]
81. Rode, C.; Peuhkuri, R.; Svennberg, K.; Time, B.; Svennberg, K.; Ojanen, T. Moisture Buffer Value of Building Materials. *J. ASTM Int.* **2006**, *4*, 1–15. [CrossRef]
82. Maaroufi, M.; Belarbi, R.; Abahri, K.; Benmahiddine, F. Full characterization of hygrothermal, mechanical and morphological properties of a recycled expanded polystyrene-based mortar. *Constr. Build. Mater.* **2021**, *301*, 124310. [CrossRef]
83. Thomas, N.L.; Birchall, J.D. The retarding action of sugars on cement hydration. *Cem. Concr. Res.* **1983**, *13*, 830–842. [CrossRef]
84. Swathi, V.; Asadi, S.S. Structural performance of hybrid fibres based concrete: Mechanical, durability and microstructural properties. *Sustain. Futur.* **2022**, *4*, 100094. [CrossRef]
85. Doumongue, B.; Limam, K.; Dany, A.Y.; Mastouri, H.; Bahi, H.; El Bouazouli, A. Analysis of rice husk concrete samples observed by scanning electron microscopy. *Mater. Today Proc.* **2023**, *72 Pt 7*, 3850–3856. [CrossRef]
86. Faso, B. Experimental Investigations on the Physical and Mechanical Properties of a Lightweight Concrete Using Oil Palm Shell as Coarse Aggregate. *J. Mater. Sci. Eng. A* **2017**, *7*, 157–168. [CrossRef]
87. Vo, L.T.T.; Navard, P. Treatments of plant biomass for cementitious building materials—A review. *Constr. Build. Mater.* **2016**, *121*, 161–176. [CrossRef]